Simulation Study on the Micro Overcharge Cycling Aging Characteristics of Lithium-Ion Batteries

Yu Lu, SHEN Wenjin, XUE Le

***Abstract*— This study systematically reveals the key aging mechanisms of nickel-cobalt-manganese ternary lithium-ion batteries under slight overcharge cycling through simulation experiments. By monitoring voltage evolution, recyclable lithium loss, localized state-of-charge variations, and lithium plating phenomena, the decisive influence of charging voltage on battery performance and lifespan was identified. Results demonstrate that the 4.2 V charging system exhibits optimal cycling stability, with a capacity retention rate significantly superior to other systems after 2000 cycles, whereas the 4.8 V system is only suitable for short-term high-power applications. Each 0.2 V increase in charging voltage accelerates capacity decay by 5–7%, reduces cycle life by 200–300 cycles, and triggers nonlinear accelerated aging in later stages. A critical voltage threshold of 4.6 V was established: above this value, irreversible dynamic evolution of the solid electrolyte interphase layer occurs, accompanied by severe electrolyte degradation and lithium dendrite initiation. These findings provide engineering guidance for lifespan prediction and safety boundary definition in high-energy-density battery systems.**

***Index Terms*— NCM ternary lithium-ion batteries; Slight overcharge cycling; Aging behavior; Charging voltage**

I. INTRODUCTION

To achieve the "Dual Carbon" strategic goals, new energy vehicles (NEVs) are globally recognized as a critical pathway and have garnered extensive attention and rapid development. Lithium-ion batteries (LIBs), characterized by high energy density, long lifespan, and environmental friendliness, are widely employed in NEVs, portable devices, and energy storage systems [1]. However, in practical applications, factors such as battery management system (BMS) malfunctions or cell inconsistency may lead to slight overcharging in individual cells. The definition of slight overcharging is determined by the battery's state of charge (SOC). Ouyang et al. [2] defined the slight overcharge range as 100% < SOC < 120%. Prolonged slight overcharge cycling can shorten battery lifespan, accelerate aging, degrade capacity and performance, and even induce thermal runaway, posing safety risks [3].

In real-world scenarios, parameters such as voltage, current, and temperature during charging/discharging are typically monitored via BMS [4,5]. However, the accuracy of this method relies on sensor sensitivity and the scientific validity of threshold settings. Furthermore, the intricate internal reactions of LIBs, coupled with fluctuating voltage patterns and the hysteresis of overcharge detection, make it challenging to identify overcharging solely through external parameters [6]. Thus, it is imperative to investigate the aging characteristics of LIBs under overcharge cycling.

Domestic and international scholars have conducted extensive research on slight overcharge-induced aging. Devie et al. [7] demonstrated that slight overcharging accelerates battery aging, and LIBs may persistently undergo slight overcharge cycling in practical use. J.L. Liu et al. [8] explored the aging mechanisms of NCM ternary LIBs under varying cutoff voltages, revealing that cells can tolerate slight overcharging below 4.60 V (normal operating range: 2.75–4.40 V). At 4.40 V cycling, the primary aging mechanism involves gradual electrode degradation due to electrochemical stress from cycling, leading to irreversible active material loss. M.J. Yang et al. [9] investigated the impact of slight overcharging on $LiFePO_4$ battery aging and thermal runaway. Results indicated that high cutoff voltages (4.50 V, nominal range: 2.30–3.65 V) exacerbate active lithium loss, accelerating capacity fade. However, moderately increasing the upper cutoff voltage to 4.00–4.20 V may suppress aging. Wang Yinfei et al. [10] studied the aging mechanisms of $LiFePO_4$ batteries under slight overcharge conditions, concluding that active lithium loss and active material degradation dominate aging, with lithium loss becoming predominant as the cutoff voltage rises.

Existing studies on slight overcharge cycling aging primarily focus on voltages ≤4.4 V, leaving high-voltage regimes (>4.4 V) underexplored. This study extends the overcharge conditions to 4.8 V, conducts in-depth electrochemical analyses, and investigates the loss of recyclable lithium, SEI layer thickening, electrolyte volume fraction changes, and lithium plating phenomena, thereby addressing the research gap in long-term high-voltage aging studies.

II. SIMULATION OF AGING MECHANISMS

A. SEI Layer Formation

A thin film forms on the electrode surface during the initial charge-discharge cycles of a new battery [11]. This process involves the reduction of lithium salts in the electrolyte and reactions of decomposed electrolyte solvents and oxides at the electrode surface. The byproducts at the anode/electrolyte interface undergo heterogeneous nucleation and growth mechanisms, gradually forming a highly dense solid electrolyte interphase (SEI) layer.

The SEI layer critically influences the performance and lifespan of lithium-ion batteries. SEI thickening induces:

a) Reduced recyclable lithium;
b) Increased internal resistance, limiting lithium-ion diffusion;
c) Decreased porosity.

The dynamic growth of the SEI layer involves multi-physics coupling effects, with existing theoretical models often

Manuscript received March 29, 2025

Yu Lu, School of Transportation Engineering, Dalian Jiaotong University, Dalian, China
Wenjin, School of Transportation Engineering, Dalian Jiaotong University, Dalian, China
Le, School of Transportation Engineering, Dalian Jiaotong University, Dalian, China

employing reduced-order equations to approximate its non-equilibrium evolution. As shown in Eq. (1):

$$S + Li^+ + e^- \rightarrow P_{SEI} \#(1)$$

In the equation, S represents the electrolyte solvent acting as a reactant, primarily ethylene carbonate (EC), while P_{SEI} I denotes the reaction products.

The generation of P_{SEI} leads to:

a) Loss of recyclable lithium in the battery;
b) Increased resistance of the SEI layer [12,13];
c) Reduced electrolyte volume fraction in the anode.

Considering the diffusion-limite d nature of SEI formation, lithium intercalation in graphite accelerates aging, and reduction reactions proceed faster at lower potentials. This behavior can be described by reaction kinetics equations[14]:

$$i_{loc,SEI} = -(1 + HK)\frac{Ji_{loc,1C,ref}}{\exp\left(\frac{\alpha\eta_{SEI}F}{RT}\right) + \frac{q_{SEI}fJ}{i_{loc,1C,ref}}} \# \quad (2)$$

In the equation, $i_{loc,SEI}$ (A/m²) represents the local current density on the graphite anode particle surface; J (dimensionless) is the dimensionless exchange current density for parasitic reactions; f （1/s）denotes the lumped dimensionless parameter based on SEI layer properties; HK (dimensionless) is the dimensionless graphite expansion factor function, which equals zero during discharge; $i_{loc,1C,ref}$ （A/m²）is the reference local current density at 1C discharge rate; $\alpha\alpha$ (dimensionless) represents the charge transfer coefficient for the electrochemical reduction reaction; $\eta_{SEI}(V)$ is the overpotential induced by SEI formation; $F(C/mol)$ is the Faraday constant; and $q_{SEI}(C/m^2)$ denotes the charge loss due to SEI formation.

Additionally,

$$\frac{\partial c_{SEI}}{\partial t} = \frac{v_{SEI} i_{loc,SEI}}{nF} \#(3)$$

where c_{SEI}(mol/m³) is the SEI concentration, and v_{SEI} is the stoichiometric coefficient of SEI species in the reaction.

$$q_{SEI} = \frac{Fc_{SEI}}{A_v} \#(4)$$

where $A_v(1/m)$ is the electrode surface area.

The SEI layer thickness $\delta_{film}(\Omega \cdot m^2)$ can be expressed as:

$$\delta_{film} = \frac{c_{SEI}M_P}{A_v\rho_P} + \delta_{film,0} \#(5)$$

where $M_P(kg/mol)$ is the molar mass, $\rho_P(kg/m^3)$ is the SEI density, and $\rho_P(kg/m^3)$ is the initial SEI thickness at t=0, set to 1 nm.

The SEI layer resistance $R_{film}(\Omega \cdot m^2)$ is given by:

$$R_{film} = \frac{\delta_{film}}{K_{SEI}} \#(6)$$

where $K_{SEI}(s/m)$ is the lithium-ion conductivity of the SEI layer.

B. Lithium Plating

During overcharging, metallic lithium deposits on the anode surface due to insufficient anode capacity. Lithium plating leads to significant lithium-ion loss, increased internal resistance, and accelerated capacity fade. Severe cases may result in lithium dendrite growth, which can pierce the separator, cause internal short circuits, and trigger thermal runaway. Lithium plating is a critical factor in studying lithium-ion battery aging. To simulate lithium plating, the empirical Arrhenius equation [15] is applied:

$$K = Ae - \frac{Ea}{RT} \#(7)$$

where K (s^{-1}) is the reaction rate constant; A (s^{-1}) is the pre-exponential factor; Ea（J/mol）is the activation energy; R （J/(mol·K)）is the universal gas constant; and T（K）is the absolute temperature.

$$(\tau - 1)S + (\tau - 1)Li(s) \rightarrow (\tau - 1)P_{SEI} \#(8)\#$$

Substituting into (1), we derive:

$$\tau S + Li^+ + e^- + (\tau - 1)Li(s) \rightarrow \tau P_{SEI} \quad (9)$$

III. SIMULATION MODEL

A. P2D Electrochemical Model

The lithium-ion electrochemical model is established based on mass conservation, charge conservation, and energy conservation. This model simulates the entire electrochemical process—including electron transport, ion migration, and electrode reactions—occurring at the microscale of electrodes across temporal and spatial dimensions. The most renowned framework is the pseudo-two-dimensional (P2D) model proposed by Newman [16]. This model incorporates two dimensions:

a) Lateral Dimension: Typically includes three components—electrodes (cathode and anode), separator, and electrolyte—with some extensions incorporating current collectors.
b) Radial Dimension: Treats the electrode's active materials as homogenized spherical particles.

Since the model accounts only for lateral variations, it is also termed a one-dimensional model. The model construction adheres to three fundamental assumptions:

a) Electrode materials are composed of spherical particles.
b) Double-layer effects are neglected.
c) Current collectors exhibit sufficiently high conductivity, rendering electrochemical variations along the y-axes and z-axes negligible. Thus, electrochemical features are analyzed solely along the x-axis.

Under these assumptions, a one-dimensional isothermal model for lithium ions is derived, as illustrated in Fig.1

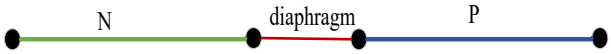

Fig 1 One-dimensional electrochemical model

B. Model Parameters

This study employs a ternary pouch-type lithium-ion battery (NCM) as the research subject. Its parameters are detailed in Tab.1 and Tab.2 [17].

Tab.1 Basic Battery Parameters

Parameter	Value
Rated Capacity	20 Ah
Charge Limit Voltage	4.2 V
Discharge Cut-off Voltage	2.8 V

Tab.2 Model parameters

Parameter	Cathode	Separator	Anode
Bruggeman Tortuosity Exponent	2.98	2.15	2.5
Initial Electrolyte (mol/m³)	—	1200	—
Maximum Anode	49000	—	31507

Capacity (mol/m³)			
Initial Li^+ Concentration (mol/m³))	4900	—	29932
Electrolyte Phase Volume Fraction	0.40	0. 60	0.30
Electrode Phase Volume Fraction	0.53	—	0.70
Thickness (μm)	85	20	11
Particle Radius (μm)	2.50	—	2.5
Conductivity (S/m)	—	100	—
Diffusion Coefficient (m²/s)	5×10^{-13}	—	1.45×10^{-13}
Density (kg/m³)	2328.5	492.16	1347.33
Specific Heat Capacity (J/(kg·K))	1269.21	1978.16	1437.4
Thermal Conductivity (W/(m·K))	1.58	0.344	1.04

IV. DISCUSSION

a) Model Validation and Analysis

The model was simulated at 25°C under 1C and 3C discharge rates to obtain voltage curves, as shown in Fig. 2. By comparing the simulated voltage profiles with experimental data [18] during the discharge phase, the results demonstrate close alignment, preliminarily validating the model's accuracy.

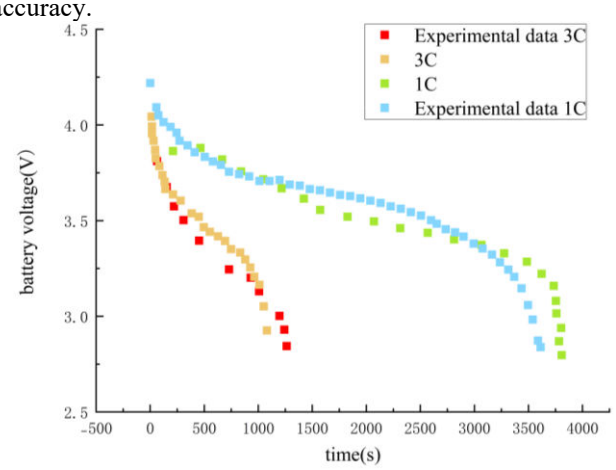

Fig. 2 Voltage changes in experiments and simulations

A 2000-cycle charge-discharge experimental framework was constructed to compare standard charging with overcharging modes (Fig. 3). The NCM battery exhibits a distinct voltage plateau in the 3.6–3.7 V range. At 4.8 V charging, the initial discharge voltage remains at 4.69 V after 2000 cycles, higher than the 4.13 V observed at 4.2 V. Increasing the charging voltage extends discharge duration, indicating enhanced energy density. All batteries terminate near 2.78 V, consistent with lithium-ion battery discharge specifications.

The slope of the discharge curve reflects internal resistance. During cycling, resistance follows a "high-low-high" trend: elevated at initial and final stages, reduced in intermediate phases. At 4.8 V, the voltage decline rate (0.00046 V/s) is 43.8% steeper than at 4.2 V (0.00032 V/s), confirming intensified polarization effects under high voltages. Similarly, the 4.6 V decay rate exceeds 4.4 V by 10.8%, validating the positive correlation between voltage elevation and accelerated capacity fade. As cutoff voltages increase, variations in discharge duration across cycles diminish, suggesting reduced influence of internal resistance and dominance of polarization losses in capacity degradation.

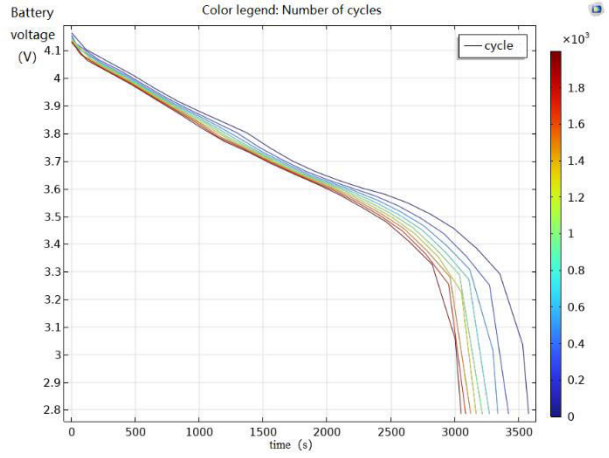

(a)

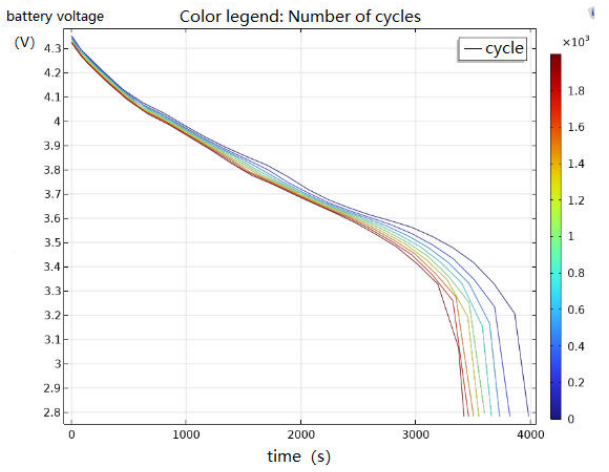

(b)

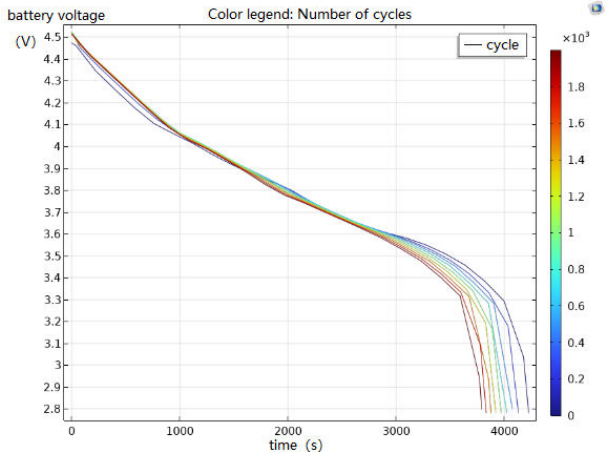

(c)

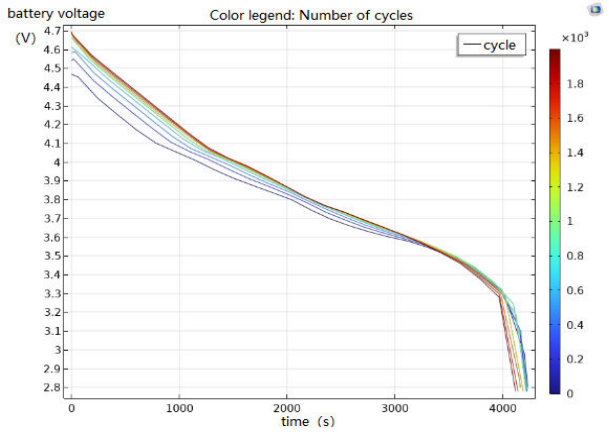

(d)

Fig. 3 (a) 4.2V (b) 4.4V (c) 4.6V (d) 4.8V charging curve

b) Overcharge-Induced Aging Analysis

Lithium-ion batteries undergo aging under both normal and abusive conditions. Dubarry et al. [19] classified aging mechanisms into three modes: Loss of Conductivity (LOC), Loss of Lithium Inventory (LLI), and Loss of Active Material (LAM).

a) LOC: Conductivity degradation originates from interfacial failures such as electrochemical corrosion of current collectors and binder delamination. This directly manifests as exponential growth in ohmic polarization resistance and a significant increase in heat generation.

b) LLI: Lithium inventory loss arises from multi-scale coupled side reactions, including lithium plating within graphite layers, lithium dendrite growth, dynamic reconstruction of the solid electrolyte interphase (SEI) layer, and continuous electrolyte degradation. These processes drive a power-law increase in SEI layer impedance with cycling.

c) LAM: Active material loss is dominated by structural destabilization of electrode materials, characterized by mechanical fracture of active particles, phase transitions in layered structures, and disintegration of the conductive binder network. These physicochemical degradations ultimately lead to irreversible loss of effective lithium intercalation sites.

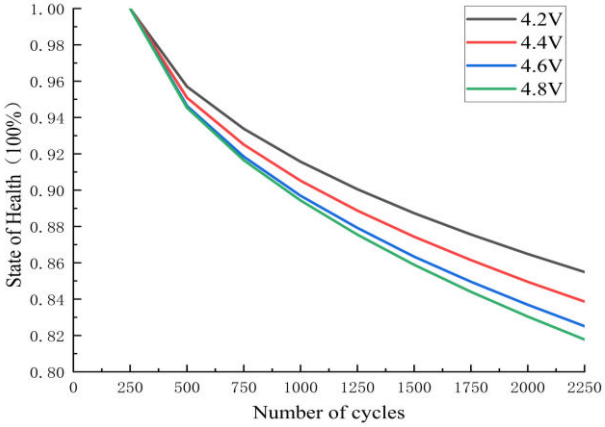

Fig. 4 Battery health at different voltages for charging cycles

As shown in Fig. 4, after 2000 cycles at 4.2 V, the lithium-ion battery exhibits a state of health (SOH) of 0.8649, corresponding to a total capacity degradation of 13.5% and an average degradation rate of 6.8% per thousand cycles. In contrast, after 2000 cycles at 4.8 V, the SOH drops to 0.8304 (total degradation: 17.0%, average rate: 8.5% per thousand cycles). The accelerated voltage decline observed in early discharge stages aligns with capacity fade, reflecting increased internal resistance due to active lithium loss and SEI layer thickening.

Tab. 3 Comparison of end-of-life predictions

Voltage (V)	End of Life (Cycle Count)	Reduction vs. 4.2 V
4.2V	~3000±50	-
4.4V	~2750±50	8.3%
4.6V	~2500±50	16.7%
4.8V	~2350±50	21.7%

As summarized in Tab. 3, lithium-ion batteries charged at 4.2 V reach their end of life (EOL) after 3000 cycles, defined as a state of health (SOH) of 80%. In contrast, under 4.8 V charging, the EOL occurs significantly earlier at 2350 cycles, corresponding to a 21.7% reduction in cycle life compared to the 4.2 V baseline.

The dynamic growth of the SEI layer is a dominant aging mechanism. Variations in the SEI layer's potential drop correlate with SOH degradation, serving as an indirect indicator of battery health. For instance: At 4.2 V, gradual SEI thickening contributes to controlled capacity fade. At 4.8 V, accelerated SEI evolution exacerbates lithium loss and resistance rise, hastening EOL. Thus, monitoring the SEI layer's electrochemical potential is critical for early detection of aging trends and optimizing charging protocols.

From Figure 5, it can be observed that the absolute potential drop accelerates significantly with increasing charging voltage. After 2000 cycles, the potential drop at 4.8 V (0.0448 V) is 20.8% higher than that at 4.2 V (0.0371 V), indicating that higher voltages markedly intensify side reactions in the SEI layer.

The growth in SEI potential drop stems from electrolyte decomposition and SEI layer thickening, as reaction kinetics become more vigorous under high-voltage conditions. Concurrently, the increase in SEI potential drop reflects a rise in SEI impedance, which elevates lithium-ion transport resistance and directly correlates with capacity fade (SOH degradation).At 4.8 V, the highest SEI potential drop (0.0448 V) corresponds to the lowest SOH (0.8304), confirming SEI deterioration as a primary driver of capacity loss.

At 4.2 V, the lowest SEI potential drop (0.0371 V) aligns with the highest SOH (0.8649), demonstrating superior SEI stability under standard voltage conditions.

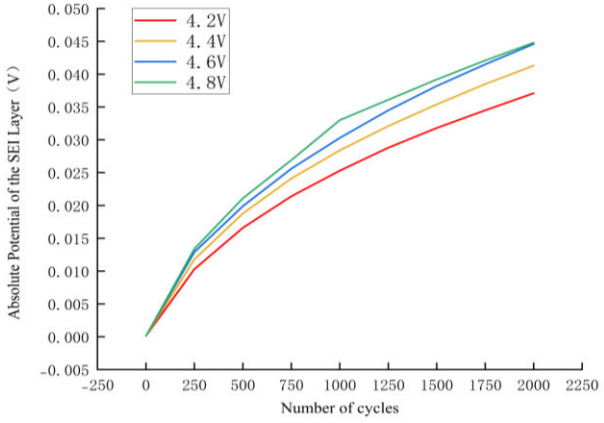

Fig. 5 Absolute Value of the SEI Potential Difference between the Negative Electrode and the Membrane

The electrolyte, responsible for lithium-ion transport between electrodes, plays a critical role in chemical-to-electrical energy conversion. Battery aging is closely linked to changes

in electrolyte volume fraction, as illustrated in Fig. 6. Initially, all cells exhibit an electrolyte volume fraction of 0.444 under identical experimental conditions. After 2000 cycles: At 4.2 V, the electrolyte volume fraction decreases to 0.292 (34.2% reduction). At 4.8 V, it drops to 0.257 (42.1% reduction), representing a 23% greater decline compared to 4.2 V.

The electrolyte consumption rate at 4.8 V is ~25% faster than at 4.2 V, underscoring the pronounced electrolyte decomposition and side reactions under high voltages.

The reduced electrolyte volume fraction diminishes effective lithium-ion transport pathways, increasing internal resistance. This aligns with the observed SEI potential drop trends (e.g., 0.0448 V at 4.8 V) and explains the accelerated capacity fade (SOH = 0.8304 at 4.8 V vs. 0.8649 at 4.2 V, a 3.5% lower SOH). Notably, beyond 1500 cycles at voltages ≥4.6 V, the divergence in electrolyte volume fraction widens, signaling the onset of accelerated electrolyte-driven degradation mechanisms.

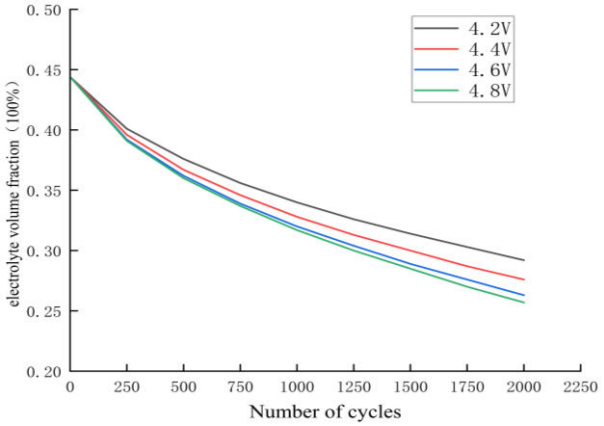

Fig. 6 Volume concentration of electrolyte at the anode-separator interface of lithium batteries

When lithium plating occurs, the anode potential drops to 0 V, initiating lithium deposition kinetics. Monitoring anode potential is thus a critical method for detecting lithium plating. Fig. 7 illustrates the anode potential of lithium-ion batteries during the 2000th cycle under varying voltages: At 4.5 V: The anode potential rapidly declines to 0.01 V, briefly entering a negative range (−0.01 V), indicative of mild polarization. At 4.6–5.0 V (overcharging): Lithium plating initiates at the anode-separator interface. At 5.0 V, severe potential fluctuations (−0.058 V to 0.90 V) reflect repeated lithium dendrite growth and dissolution, posing a risk of separator penetration and internal short circuits. Above 4.8 V: A sharp potential drop correlates with accelerated electrolyte oxidative decomposition, accompanied by gas evolution that heightens thermal runaway risks.

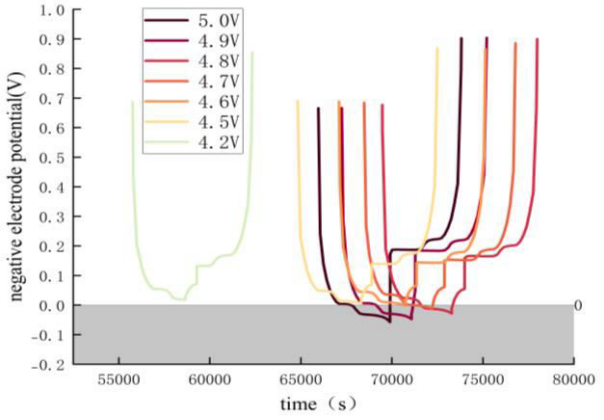

Fig. 7 Negative potential at the anode-diaphragm interface at different voltages

CONCLUSIONS

This study investigated the full-lifecycle aging behavior of NCM ternary lithium-ion batteries under slight overcharge cycling conditions through simulation experiments. By monitoring voltage evolution, recyclable lithium loss, localized state-of-charge variations, and lithium plating during overcharging, the mechanisms driving aging under slight overcharge cycling were systematically elucidated. Key conclusions are summarized as follows:

a) Voltage-Dependent Discharge Performance:

Discharge performance is strongly correlated with charging voltage. Higher voltages enhance energy density but accelerate degradation. The 4.2 V system retains optimal stability after 2000 cycles, while the 4.8 V system is suitable only for short-term high-power applications and requires targeted optimization for lifespan extension.

b) Voltage-Cycle Life Relationship:

Each 0.2 V increase in charging voltage accelerates capacity fade by 5–7% and reduces cycle life by 200–300 cycles. High voltages (>4.4 V) induce nonlinear aging during later cycles.

c) Critical Voltage Threshold:

A critical threshold of 4.6 V was identified. At voltages ≥4.6 V, irreversible dynamic evolution of the SEI layer occurs, accompanied by severe electrolyte instability and lithium dendrite initiation. Such conditions demand strict operational constraints.

d) SEI Layer Degradation:

Each 0.2 V voltage increment increases the SEI potential drop growth rate by 5–7%, resulting in a 1.5% SOH decline after 2000 cycles.

e) Multi-Dimensional Health Assessment:

A holistic health evaluation model can be developed by integrating SEI potential drop, anode interfacial potential, and capacity data. This framework provides theoretical and engineering guidance for battery safety management.

REFERENCES

[1]MIN Yueming, ZHANG Chuang, LIU Wenjie, LIU Suzh-en, XU Zhiche ng. Study on aging characteristics and failure mechanism of lithium-i on battery under slight-overcharge cycling[J]. Energy Storage Science and Technology, 2024, 13(10): 3343-3356.

[2]OUYANG M, REN D, LU L, et al. Overcharge-induced capacity fading analysis for large format lithium-ion batteries with LiyNi1/3Co1/3Mn 1/3O2+ LiyMn2O4 composite cathode[J]. Journal of Power Sources, 2015, 279: 626-635.

[3]WANG Z, YUAN J, ZHU X, et al. Overcharge-to-thermal-runaway beha vior and safety assessment of commercial lithium-ion cells with differ ent cathode materials: a comparison study[J]. Journal of Energy Chem istry, 2021,55(4):484-498.

[4]WANG P, YANG L, WANG H, et al. Temperature estimation from curren t and voltage measurements in lithium-ion battery systems[J]. Journal of Energy Storage, 2021, 34: 102133.

[5] THOMAS J K, CRASTA H R, KAUSTHUBHA K, et al. Battery monito ring system using machine learning[J]. Journal of Energy Storage, 20 21, 40: 102741.

[6]LAI Yilin. Lithium-ion battery safety warning methods review[J]. Energy Storage Science and Technology, 2020, 9(6): 1926-1932.

[7]DEVIE A, DUBARRY M, WU H, et al. Overcharge study in $Li_4Ti_5O_{12}$ ba sed lithium-ion pouch cell[J]. Journal of the Electrochemical Society, 2016, 163(13): 165–186.

[8]LIU J L，PENG W，YANG M P，et al. Quantitative analysis of aging and detection of commercial 18650 lithium-ion battery under slight ov ercharging cycling［J］. Journal of Power Sources, 2020, 445: 13075 6.

[9]YANG M J，YE Y J，YANG A J，et al. Comparative study on aging an d thermal runaway of commercialLiFePO4 /graphite battery undergoi

ng slight overcharge cycling［J］. Journal of Energy Storage, 2022，50: 104691.
[10] Wang Yinfei, Yang Zhengxin, Du Jinqiao, et al. Aging mechanism of Li-ion battery under slight-overcharge condition [J]. Battery Bimonthly, 2023, 53(5): 499-503.
[11] FONG R, SACKEN U, DAHN J R. Studies of lithium intercalation into carbons using nonaqueous electrochemical cells[J]. Journal of the Electrochemical Society, 1990, 137: 2009-2013.
[12] P. Ramadass, B. Haran, P. Gomadam, et al. Development of first principles capacity fade model for li-ion cells[J]. Electrochemical Society, 2004. 151(2)A196-A203
[13] G. Ning, R. White, and B. Popov. A generalized cycle life model of rechargeable Li-ion batteries, Electrochemical Acta, 2006, 2012–2022.
[14] H. Ekström and G. Lindbergh. A model for predicting capacity fade due to SEI formation in a commercial Graphite/LiFePO4 cell[J]. Electrochemical Society, 2015, vol 162, pp. A1003 A1007.
[15] Klippenstein, S.J., Georgievskii, Y. and Harding, L.B. Predictive theory for the combination kinetics of two alkyl radicals. Physical Chemistry Chemical Physics8(0), 2006,1133.
[16] DOYLE M, FULLER T F, NEWMAN J. Modeling of galvanostatic charge and discharge of the lithium/polymer/insertion cell[J]. Journal of the Electrochemical Society, 1993, 140(6): 1526-1533.
[17] HUANG W C. Simulation and research on thermal runaway of lithium-ion battery based on COMSOL[D]. Chengdu: Southwest Jiaotong University, 2019.
[18] REN D S, HSU H, LI R H, et al. A comparative investigation of aging effects on thermal runaway behavior of lithium-ion batteries[J]. eTransportation, 2019, vol2.
[19] DUBARRY M, TRUCHOT C, LIAW B Y, et al. Evaluation of commercial lithium-ion cells based on composite positive electrode for plug-in hybrid electric vehicle applications. Part II. Degradation mechanism under 2 C cycle aging[J]. Journal of Power Sources, 2011, 196(23): 10336-10343.